A comparison of steady, pulsating flow measurements and CFD simulations in close coupled catalysts

Arias-García, A. , Benjamin, S.F. , Zhao, H. and Farr, S.

SAE TECHNICAL PAPER SERIES

2001-01-3662

A Comparison of Steady, Pulsating Flow Measurements and CFD Simulations in Close Coupled Catalysts

A. Arias-García, S. F. Benjamin and H. Zhao
Coventry Univ.

S. Farr
ArvinMeritor Ltd.

Reprinted From: General Emissions and Gasoline Emission Control Systems (SP–1644)

The Engineering Society For Advancing Mobility Land Sea Air and Space®
SAE INTERNATIONAL

International Fall Fuels and Lubricants Meeting and Exposition
San Antonio, Texas
September 24-27, 2001

400 Commonwealth Drive, Warrendale, PA 15096-0001 U.S.A. Tel: (724) 776-4841 Fax: (724) 776-5760

ISSN 0148-7191

Printed in USA

2001-01-3662

A Comparison of Steady, Pulsating Flow Measurements and CFD Simulations in Close Coupled Catalysts

A. Arias-García, S. F. Benjamin and H. Zhao
Coventry Univ.

S. Farr
ArvinMeritor Ltd.

ABSTRACT

Performance improvements of automotive catalytic converters can be achieved by improving the flow distribution of exhaust gases within the substrate. The flow distribution is often assumed to be adequately described by measurements obtained from steady flow rigs. An experimental study was carried out to characterise the flow distribution through the substrate of a close-coupled catalytic converter for both steady and pulsating conditions on a flow rig and on a motored engine. Computational fluid dynamic (CFD) simulations were also performed. On the flow rig, the flow from each port was activated separately discharging air to different regions of the substrate. This resulted in a high degree of flow maldistribution. For steady flow maldistribution increased with Reynolds number. Pulsating the flow resulted in a reduction in flow maldistribution. Different flow distributions were observed on the motored engine when compared to composite maps derived from the rig. For the engine study significantly more flow activity was observed at the periphery of the substrate, each port contributing to the net flow. The results suggest that strong port interactions occur. CFD simulations showed qualitative agreement with measurements but underestimated the flow maldistribution.

INTRODUCTION

Catalytic converters are an effective means of reducing automotive emissions. Their performance is known to be significantly affected by the flow distribution within the catalyst monolith. Early work showed that a uniform flow distribution is highly desirable in order to enhance converter efficiency and extend catalyst durability [1-3]. However, this is rarely achieved. Converter design parameters, vehicle packaging constrains, and engine operating conditions all are crucial factors that contribute to flow maldistribution inside the catalytic converter. In particular there has recently been a move towards close coupled catalyst (CCC) designs in order to reduce light-off times. CCCs feature highly complex geometries and strongly pulsating flows. This can lead to a high degree of flow maldistribution, which needs quantifying in order to assess their likely performance.

Information on the flow distribution in catalyst monoliths has been obtained from measurements in flow rigs and engines and, more recently, from CFD simulations [1-23]. For prototype development, flow rig studies can provide useful information on the flow structure within the monolith. Rig studies may vary in complexity from steady flow evaluations to measurements made on rigs designed to represent more closely the pulsating flow environment of real engines. Measurements on engines, whilst clearly desirable, are extremely difficult to make. The question arises as to how representative steady state rig studies are for assessing the flow distribution within a real engine environment. CFD offers the prospect of simulating the flow behaviour of these systems. It is, however, important that the codes are properly validated if their results are to be used with confidence.

This paper is intended to address some of these issues by providing comparisons of flow studies performed on a close coupled catalyst under steady and pulsating flow conditions. The flow distribution across the monolith was measured on a flow rig and compared to that obtained on a motored engine. CFD simulations were also performed and are compared with the experimental data. This work represents part of a larger study which will compare these findings with measurements on firing engines.

EXPERIMENTAL METHOD

TEST RIG – The isothermal flow rig has been previously described by Benjamin et al [23] and is shown in figure 1. The test rig was supplied with compressed air from two receivers via a main valve (1). A pressure gauge (2) monitors the supply pressure, which was reduced from ~100 psi to ~20 psi by a valve (3). A second pressure gauge monitors the up-stream rig pressure (4). A filter (5) was used to avoid oil contamination. The mass flow rate was controlled by an adjustment valve (6). A safety relief valve rated at 80 psi was used to avoid damage to the rig (7). Rig pressure was monitored by a pressure gauge (8). Flow rate was measured using a viscous flow meter (VFM) (10). Up-stream of the VFM was a 50 mm flow straightener (9) used to ensure a smooth inlet to the VFM. The viscous flow meter was connected to a digital manometer FCO16 from Furness Controls. A plenum incorporating a flow straightener (11) was used to avoid swirl components in the flow and a contracting nozzle (12) produced a uniform velocity profile at the diffuser inlet under steady flow conditions. The pulsations were achieved using a pulse generator (13) of which a schematic can be seen in figure 2. When pulsating flow is required it was found necessary to incorporate a tube (14) holding flow straighteners so as to achieve uniform flow as shown in figure 3. The inlet pipe diameter, on which all Reynolds numbers were based, was 48 mm. The diffuser (15) was replaced for these experiments with a close coupled catalyst manifold as described later. On the test substrate (16) an outlet sleeve (17) was used to avoid entrainment of surrounding air.

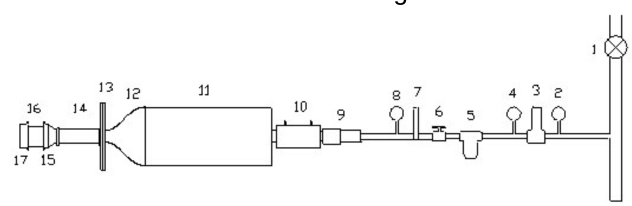

Figure 1. Schematic of iso-thermal flow rig

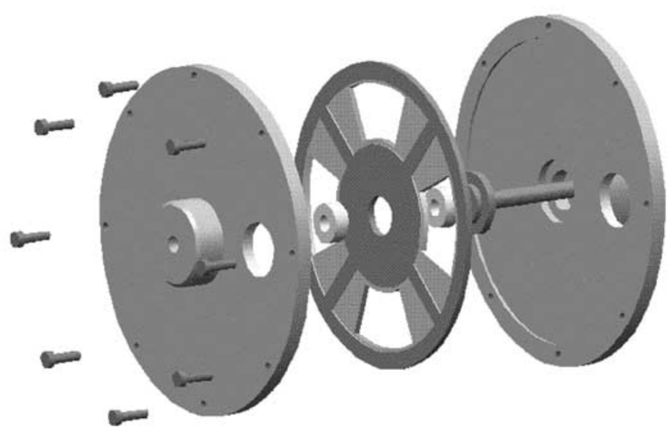

Figure 2. Exploded schematic of pulse generator.

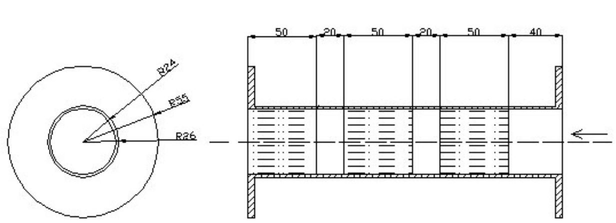

Figure 3. Schematic of flow straightener arrangement on the flow rig -arrow indicates flow direction.

FLOW DISTRIBUTION MEASUREMENTS - The flow distribution was determined by mapping velocity profiles at the rear of the substrate. For the velocity measurements a TSI IFA 300 Constant Temperature Hot Wire Anemometry (HWA) system was used, as seen in figure 4. The system comprises of a main unit with the HWA bridges, a 2D traverse and the ThermalPro software to control, acquire and analyse the data. The probes were 5 μm Tungsten/Platinum wires, calibrated using a TSI 1129 fully automatic calibration rig. The velocity profiles were measured in the outlet sleeve 30 mm downstream of the substrate. Previous work [8] showed that this distance was necessary in order to avoid the jet effect from individual monolith channels.

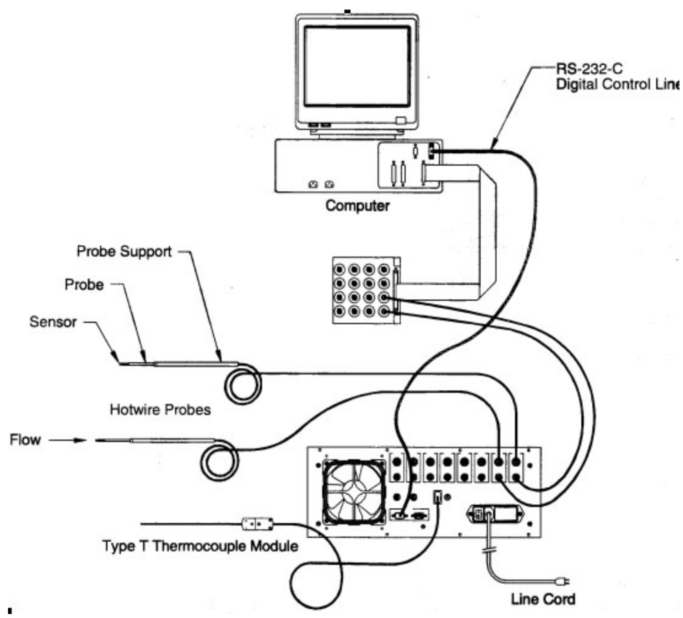

Figure 4. Overview of the IFA 300 System (Courtesy of TSI) [24]

INLET CONDITIONS - Inlet conditions at the entrance to the manifold can significantly affect the flow distribution in monolith substrates [14]. It is therefore important to ensure that they are well defined and representative of what may be expected from engines. This is equally important for the assessment of CFD simulations which require a prescription of the inlet boundary condition. The inlet velocity distribution and pulsation pattern was measured as follows. The tube accommodating the honeycomb ceramic substrates (figure 3) was extended with a sleeve. The sleeve has the same inner diameter as the tube and a length of 30mm to eliminate the jet effect caused by the pore structure of the ceramic substrate. The inlet condition was measured at the exit of the sleeve, 260mm downstream from the chopper. The sampling rate for the HWA measurements was 2000 measuring points per second, which is adequate for resolving velocity oscillations of 25 Hz. Figure 5 shows the velocity variation versus time measured at the centre of the sleeve exit and figure 6 shows the time mean velocity profiles along the horizontal and vertical centrelines at the sleeve exit for Re~60000 at 25 Hz. The figures show that with the flow straighteners in place approximately uniform flow and sinusoidal velocity pulses were produced.

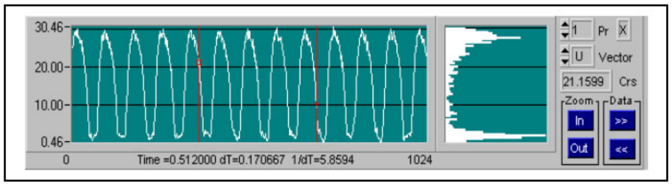

Figure 5. Instantaneous velocity at the centre of the exit sleeve of the flow straightener tube

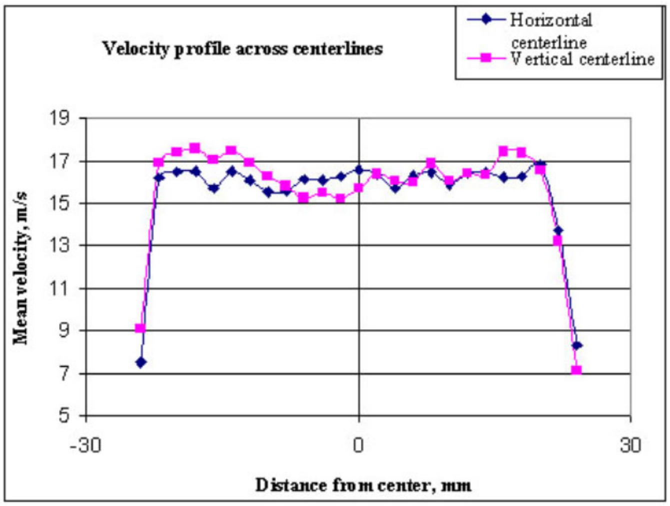

Figure 6. Velocity profile across the centrelines at the sleeve exit of flow straightener tube.

CLOSE COUPLED CATALYST – Figures 7 and 8 show the close coupled catalyst that was used. The catalyst is from a 1.4 litre engine and features four exhaust ports entering a diffuser volume (chamber) upstream of the monolith. The monolith is catalysed. It has a cell density of 400 cpsi, diameter 120mm and length 200 mm. The outlet nozzle was removed so that velocity measurements could be easily obtained across the exit to the monolith. The flow rig studies were conducted by coupling each exhaust port in turn to the flow rig whilst closing the other three ports. A short adapter was required to couple the outlet of the flow nozzle assembly to the inlet of the manifold that had a non-circular section.

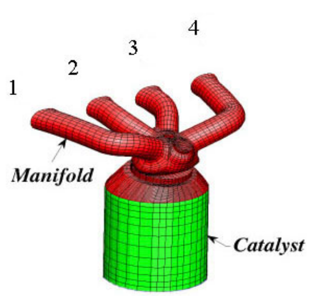

Figure 7. CCC system used for the experiments and CFD studies.

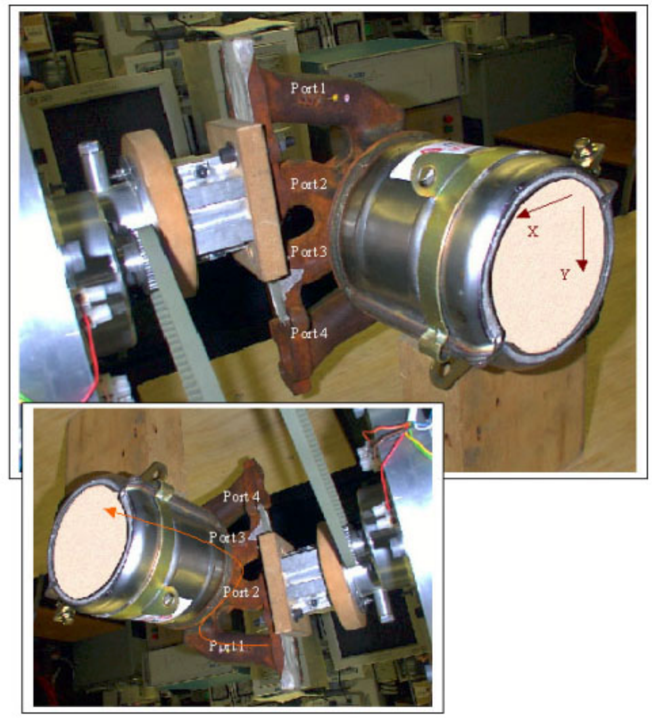

Figure 8. Manifold attached to the rig by adapter [25]. The lower view is shown for ease of comparison with measured velocity distributions (outlet sleeve omitted for clarity).

For the motored engine studies the exhaust system was taken off the engine and replaced by the manifold/catalyst assembly used on the rig. Hot wire velocity profiles were taken across the exit of the substrate.

EXPERIMENTAL PROCEEDURE - The experiments on the rig were carried out under steady and pulsating conditions for varying Re and frequencies (25 and 50 Hz). The experiments on the engine were performed under motoring conditions at 3000 rpm WOT, corresponding to 25Hz on the flow rig.

For the rig studies the mass flow rate under steady flow conditions was obtained from the viscous flow meter (VFM) which had been previously calibrated. Under pulsating flow, however, the VFM readings are unreliable and the mass flow rate was obtained by integrating the velocity profiles obtained at the substrate exit. Hence to compare steady and pulsating flow at the same flow rate the following procedure was adopted. Each pulsating flow experiment was conducted with a VFM setting approximating the required condition. The mass flow rate was then obtained from integration of the velocity maps at the substrate exit and the steady flow experiment was then performed at the appropriate VFM setting.

Flow velocities were measured over a grid of points at the substrate exit. Except where stated mapping at the outlet was made by means of approximately a thousand point measurements, i.e.; intervals of 2.5mm were used across both X and Y axes (see figure 8) with the outlet diameter being 120mm. The mass flow rate calculations were made assuming uniform velocity within each 6.25mm^2 measurement area.

Once the experimental work on the rig was completed experiments were carried out on the engine under motoring conditions. The velocity at the exit of the monolith was mapped using HWA at intervals of 2.5 mm across the X and Y directions

EXPERIMENTAL RESULTS

STEADY FLOW RIG - Figure 9 shows normalised velocity distributions from all ports for a Re of approximately 75000. The colour scale represents normalised velocities (i.e., the velocity at each point has been divided by the mean velocity through the substrate). Because of the symmetry of the manifold the flow distributions from ports 1 and 4, the outboard ports, are mirror images as are the distributions from the two inner most ports 2 and 3. All distributions feature small crescent shaped areas of higher velocity, the velocity magnitudes being greater for the inner two ports and positioned more centrally. There are also secondary bands of higher velocities observed towards the periphery, which tend to merge with the aforementioned crescent shaped areas for the outboard ports. Clearly the flow is highly maldistributed. The flow from the ports separates as it enters the diffuser volume. As the jets travel across the chamber they impinge across a small area of the substrate causing a local pressure rise due to the high monolith resistance. A lateral pressure gradient results causing significant radial flow (jet spreading). As this radial flow approaches the diffuser wall it stagnates, the pressure increases thus forcing more flow through the outermost channels. This is the origin of the secondary peripheral bands of high velocity. The location of the primary jet impingement determines the magnitude of these secondary peaks. For ports 2 and 3, where the jet impinges more centrally, less of the radial flow reaches the wall and so the secondary peak is reduced. There is also apparently a significant swirl component associated with the flow, the swirl axis being perpendicular to the substrate face. For example, the flow map of port 4 shows the intense flow area near the periphery is blown counter-clockwise relative to the more centrally located high velocity area, i.e. the radial flow has a greater opportunity to swirl around the chamber before entering the monolith. It is also highly likely that there are "tumble" vortices generated by the individual inboard ports, especially in the region near the wall where detachment occurs.

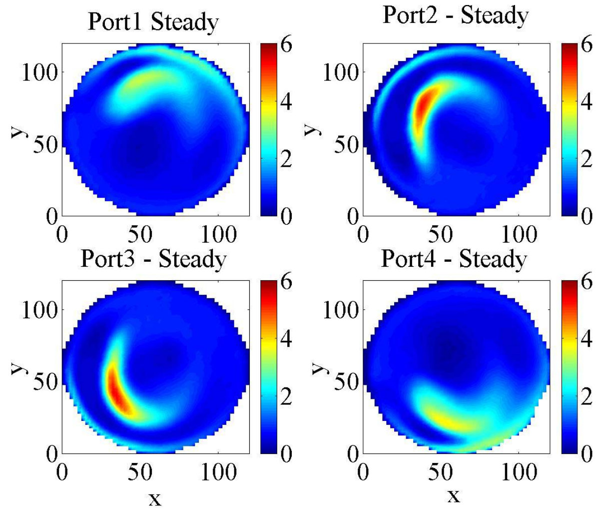

Figure 9. Velocity distribution normalised by the mean velocity, steady state. Mass flow rate and Reynolds number, port1: 0.0479kg/s and ~ 73,000; port2: 0.0488kg/s and ~ 75,000; Port3: 0.0492kg/s and ~ 75,000; port4: 0.0496kg/s and ~ 76,000.

Figure 10 shows the normalised velocity distributions for varying flow rates obtained from port 3. A coarser mesh was used in the upper part of the domain for two of the flow rates where less resolution was required, as was the case similarly in figure 12. The flow maldistribution increases with Re as has been previously observed for axi-symmetric systems [13].

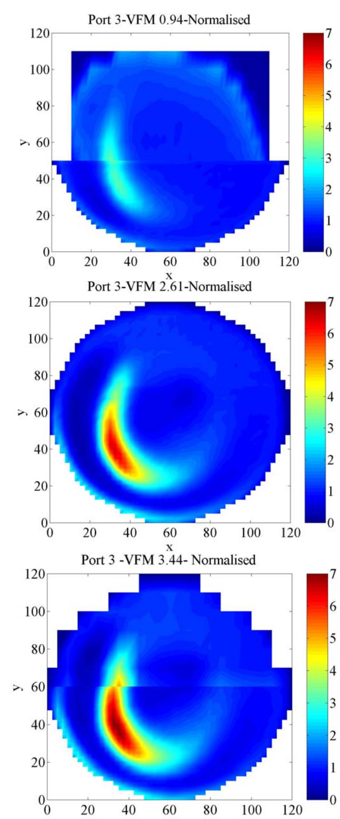

Figure 10. Effect of Re. Velocity distribution normalised by the mean velocity, steady state. Reynolds numbers ~ 20,000, 60,000 and 80,000 respectively.

PULSATING FLOW RIG - Figure 11 shows the velocity distributions at 25 Hz for each port at flow rates similar to those used in the steady flow experiment (figure 9). Maximum velocities observed in the steady and pulsating flow cases are 15 and 12 m/s respectively. The flow is overall less maldistributed at 25 Hz

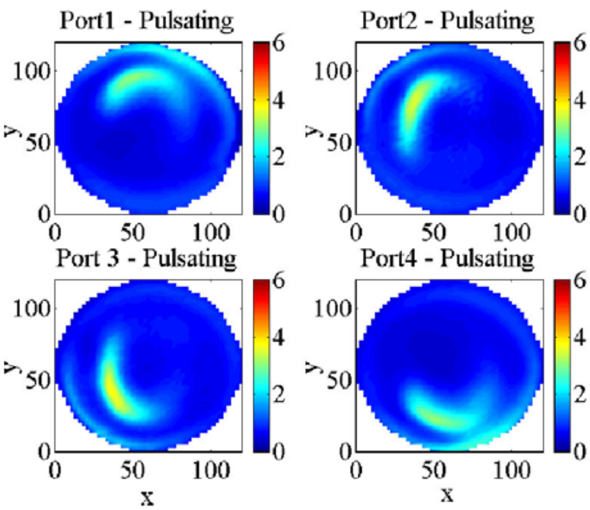

Figure 11. Velocity distribution normalised by the mean flow for four ports with pulsating flow, 25Hz. Mass flow rate and Reynolds number, port1: 0.0458kg/s and ~ 70,000; port2: 0.0468kg/s and ~ 72,000; Port3: 0.0446kg/s and ~ 68,000; port4: 0.0444kg/s and ~ 68,000.

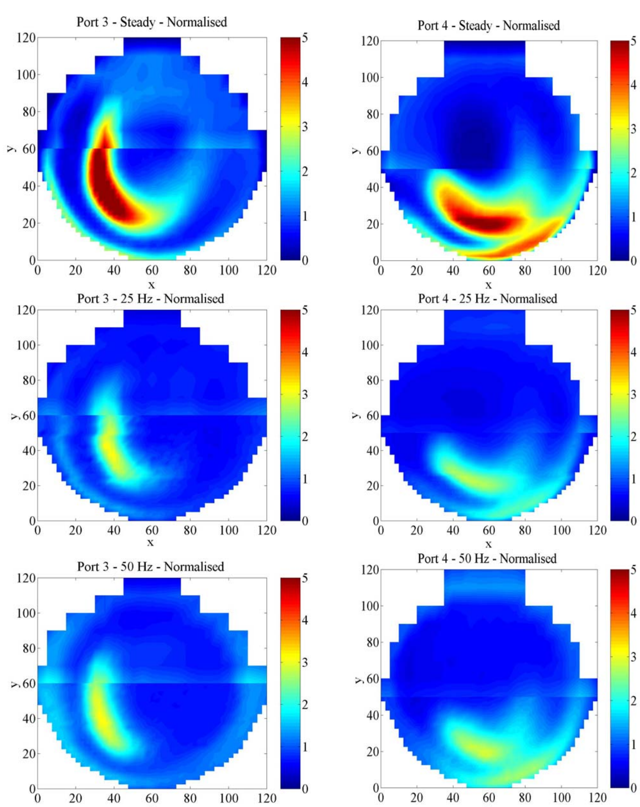

Figure 12. Frequency study for ports3 and 4. Velocity distribution normalised by the mean flow. Mass flow rate ~ 0.044kg/s; Re ~ 68,000.

Figure 12 illustrates the effect of frequency for ports 3 and 4. The patterns for each port are similar for all three cases. Pulsating the flow, however, reduces the flow maldistribution significantly. As pulsation frequency doubles the flow is slightly less maldistributed. In particular, for port 4 at the higher frequency, the two high velocity regions merge.

In order to compare with the motored engine experiment, the individual contour maps of the four ports in figure 11 were combined as follows. In the rig experiment, the velocity at every point was averaged over a continuous data acquisition period, whilst in the engine experiment, each port only contributes a quarter of the period in one cycle. So firstly every point in the individual maps was divided by 4. Because there were slight differences of mass flow rate among the four maps, every point in port 1, 2 and 3 was corrected to be on the same basis as port 4 by multiplying by a factor Ci [Ci=(mass flow rate of port 4)/(mass flow rate of port i)]. Finally, by summing up every point, figure 13 was formed. The flow pattern shows the four crescent-shaped areas merging to form a band of high intensity flow.

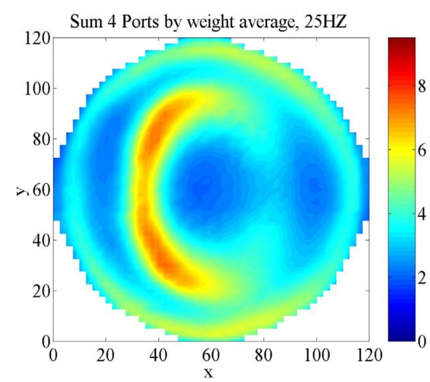

Figure 13. Cumulative velocity map (m/s) obtained with pulsating flow, pulsating frequency is 25Hz.

MOTORED ENGINE STUDY - In order to compare the rig with the engine studies the manifold was attached to the engine. The same refined mesh as in the rig studies was applied and measurements were taken at the exit of the substrate at 3000 rpm, WOT, with a mass flow rate of 0.036 Kg/s.

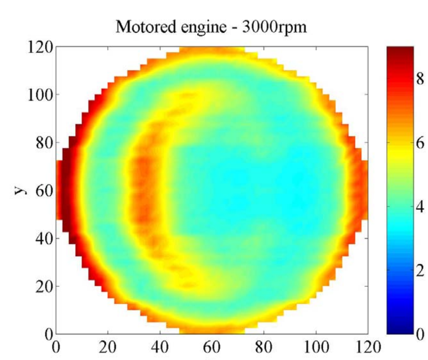

Figure 14. Velocity map (m/s) from the motored engine.

The flow pattern measured from the motored engine (figure 14) is different from the composite map obtained from the rig experiment (figure 13). The centrally located band in figure 13 is reduced in intensity and is more diffuse for the engine study and there are higher velocity flow regions on the periphery of the substrate, especially on the side furthest from the engine. It is thought that the reason for this difference is the interaction of the flow from the individual cylinders inside the diffuser volume. In the engine the four ports open in the firing order 1-3-4-2, which will cause a strong interaction between them. For instance, the flow from exhaust port 1 would certainly be pushed from behind by the flow from port 3 as would also be the case with ports 4 and 2. This may be the cause of the flow maxima observed at the substrate periphery furthest from the engine. Swirl and tumble will also serve to enhance port interactions. To gain some insight into this, pulse profiles from the motored engine were obtained by taking time resolved measurements at 5 points across the centreline of the substrate (y~60mm in figure 14). Figure 15 shows the average velocity across this centreline and the positions where pulse profiles were obtained.

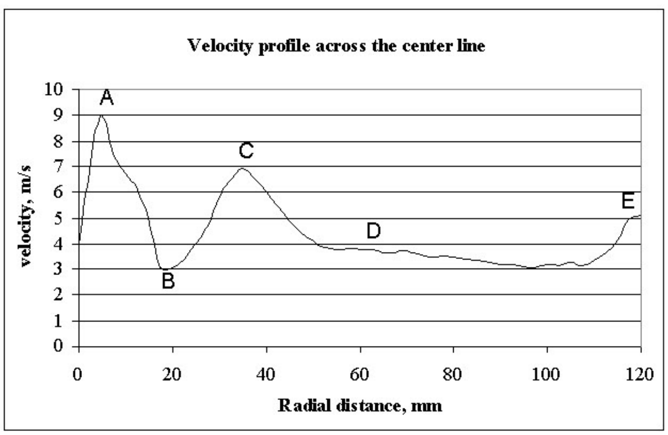

Figure 15. Velocity profile across the substrate centre line, y~60mm in figure 14. The x-coordinate represents the diameter from wall (0 mm) to the opposite wall (120 mm).

Figure 16 shows the instantaneous velocities. The time period between the two red lines in figure 16 is about 0.08s, corresponding to 2 engine cycles at 3000 rpm. In general, distinct pulse shapes can be seen at all locations although their frequency and regularity varies significantly. At point C four regular pulses are observed and these might reasonably be assumed to be associated with the pulses from the two inboard ports, 2 and 3. At point D eight regular pulses are observed suggesting all ports are contributing to the flow in this region. At points B and E pulsed flow is evident but appears less regular, the lower velocities at point B making it particularly difficult to discern the pulse behaviour. At point A the pulsing is quite pronounced and suggests all ports are contributing equally in this region. The reasons behind this are not known but would appear to be associated with strong port interactions and complex swirl motions. Finally mention should be made that the flow rate deduced from the integrated velocity profiles was approximately 40% higher than that recorded on the engine VFM. Part of this discrepancy may be due to engine / vibration problems which are estimated to cause an error of ~ 0.3 m/s in the HWA readings. A further possibility is that strong port interactions and complex recirculating flows within the diffuser volume are producing backflow through the catalyst, which cannot be detected by HWA sensors. Only directionally sensitive measurement techniques e. g. laser doppler anemometry (LDA) or CFD transient simulations will be able to resolve this.

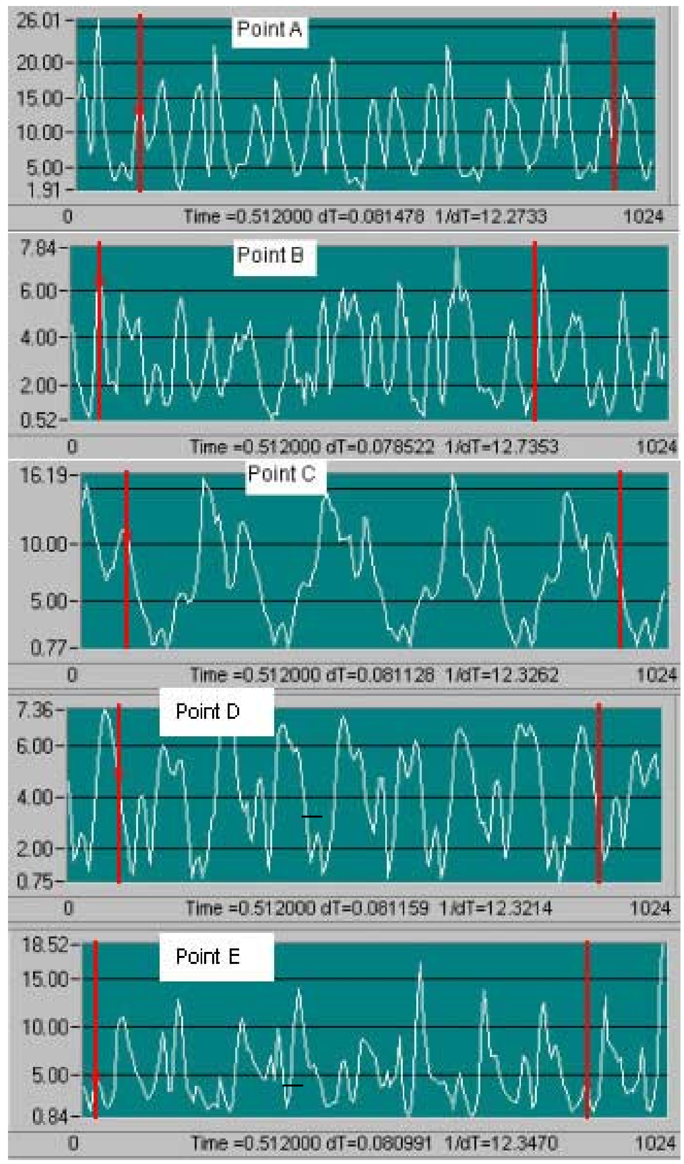

Figure 16. Pulse shapes at the points defined in figure 15

CFD PREDICTIONS

CFD analysis was performed using the STAR-CD computer code. The model used was similar to that shown in figure 7. It comprised of about 250,000 cells and was run as a series of four steady state simulation for each individual port at Re ~ 20000. The high Re number k-ε model was used and uniform flow was assumed at port inlet. The substrate was modelled as a “porous” medium with resistance based on the Hagen-Poiseuille (H-P) relationship for laminar flow in channels The predicted velocity maps at exit from the substrate are shown in figure 17. These can be compared with velocity measurements obtained from the flow rig shown in figure 18. The grid resolution in figure 18 was 5mmx5mm but is believed to be sufficiently fine for the purpose of comparison. It should be noted that the orientation of these figures is different to that shown earlier.

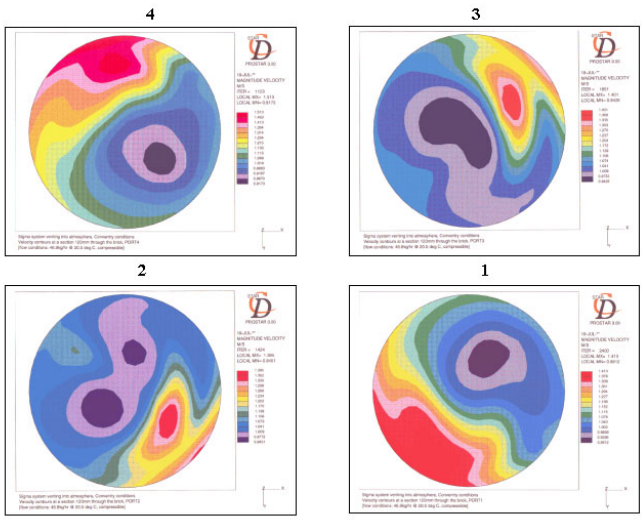

Figure 17. CFD predictions, Re~20000. Velocity magnitude beside the colour bar is from about 0.8 to 1.4 m/s.

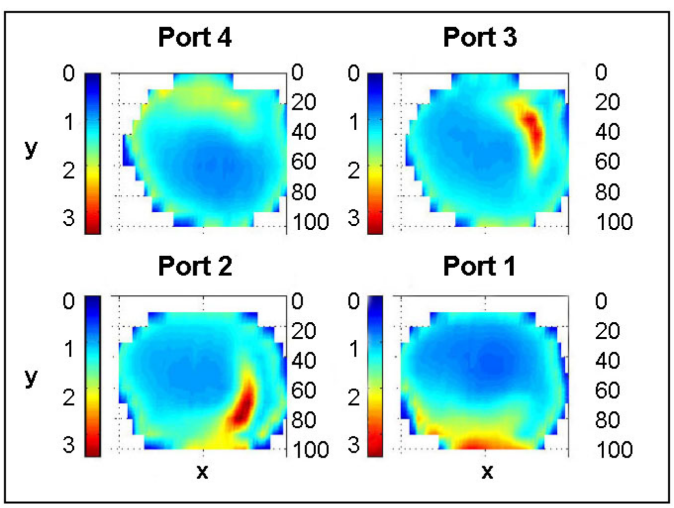

Figure 18. Velocity map of the four ports using HWA. Velocity in m/s, co-ordinates in mm, Re ~ 20,000.

Although the distribution of the flow shows a similar pattern between experiment and CFD, the latter underestimates the velocity maxima. The maximum velocity for the experimental work is about 3 m/s and in the case of CFD is approximately 1.5 m/s. It is believed that this is partly attributable to the fact that flow losses due to monolith entrance effects have not been included in the model [26]. This is the subject of ongoing research.

CONCLUSION

- Flow rig studies on a close coupled catalyst have been performed with each port blown separately for steady and pulsating flow conditions. For each port significant flow maldistribution was observed at the rear of the monolith substrate with the flow field generally featuring two areas of high velocity. The steady flow maldistribution increased with Re. Pulsating the flow resulted in a reduction in flow maldistribution.

- Tests on a motored engine showed that the flow distribution observed at the rear of the substrate was significantly different to that observed from the composite flow derived from the rig studies. It is conjectured that substantial port flow interference is occurring.

- There is only qualitative agreement between CFD steady state simulations and experiment. CFD underestimates the velocity magnitude by about 50% and hence the flow is predicted to be more uniform. It is suggested that this is partly attributable to the fact that entrance effects have not been included in the model.

ACKNOWLEDGMENTS

We would like to thank Colin Haywood and Keith Smith from Coventry University for assistance with the experiments.

REFERENCES

1. Howitt, J. S., Sekella, T. C., “Flow Effects in Monolithic Honeycomb Automotive Catalytic Converters”, Society of Automotive Engineers, Automotive Engineering Congress, Detroit, Mich. February 25-March 1, 1974. SAE Paper No.740244.
2. Lemme, C. D., Givens, W. R., “Flow Through Catalytic Converters – An Analytical and Experimental Treatment”, February 25-March 1, 1974. SAE Paper No.740243.
3. Comfort, E. H., “Monolithic Catalytic Converter Performance as a Function of Flow Distribution”, The American Society of Mechanical Engineers, 1974.
4. Wendland, D. W. and Matthes W.R. Visualization of Automotive Catalytic Converter Internal Flows SAE paper 861554, 1986
5. Jorgensen, N., Davies, M.J., Dewhurst, S. J., and Goatcher, T., “Visualising Flow Distributions Through Catalytic Converters” 25th International Symposium on Automotive Technology and Automation, 1992

6. Will, N. S., Bennett, C. J., "Flow Maldistributions in Automotive Converter Canisters and their Effect on Emission Control", SAE Paper No.922339.
7. Weltens H., Bressler H., Terres F., Neumaier H. and Rammoser D., Optimisation of catalytic converter gas flow distribution by CFD. SAE paper 930780, 1993.
8. Clarkson, R. J., "A Theoretical and experimental study of automotive catalytic converters", PhD Thesis, Coventry University 1995.
9. Wendland, D. W., Kreacher J.E. and Andersey E. Reducing Catalytic Converter Pressure Loss with Enhanced Inlet –Header Diffusion SAE paper 952398 SP-1120 pp13-23, 1995
10. Zhao, F-Q., Li, L., Xie, X., Lai, M-C., "An Experimental Study of the Flow Structure Inside the Catalytic Converter of a Gasoline Engine", SAE Paper No.950784.
11. Hawang, K., Lee, K., Mueller, J., Stuecken, T., Schock, H. J., "Dynamic Flow Study in a Catalytic Converter Using Laser Doppler Velocimetry and High Speed Flow Visualisation", International Congress and Exposition, Detroit, Michigan, February 27-March 2, 1995. SAE Paper No.950786.
12. Bressler, H., Rammonser, D., Neumaier, H., Terres, F., "Experimental and Predictive Investigation of a Close Coupled Catalyst Converter with Pulsating Flow", Heinrich Gillet GmbH & Co.1996. SAE Paper No 960564
13. Benjamin S. F., Clarkson R. J., Haimad N. and Girgis N. S.(1996) An experimental and predictive study of the flow in axisymmetric automotive exhaust catalyst systems SAE Transactions, Vol. 105, Journal of Fuels and Lubricants, Section 4, pages 1008-1019
14. Haimad N A theoretical and experimental investigation of the flow performance of automotive catalytic converters. . PhD thesis, Coventry University, 1997.
15. Jeong S.J. and Kim T. H. CFD investigation of the 3-Dimensional Unsteady Flow in the Catalytic Converter SAE paper 971025, 1997
16. Zhao, F-Q., Bai, L., Liu, Y., Chue, T-H., Lai, M-C., "Transitient Flow Characteristics Inside the Catalytic Converter of a Firing Gasoline Engine", International Congress and Exposition, Detroit, Michigan, February 24-27, 1997. SAE Paper No.971014.
17. Park, S-B., Kim, H-S., Cho, K-M., Kim, W-T., "An Experimental and Computational Study of Flow Characteristics in Exhaust Manifold and CCC (Close-Coupled Catalyst), SAE Paper No.980128.
18. Bai, L., Zhao, F-Q., Liu, Y., Lai, M-C., Lee, K-S., "Transient Flow and Pressure Characteristics inside a Close-Coupled Catalytic Converter", Society of Automotive Engineers, Inc., 1998.SAE Paper No.982548.
19. Park, S-B., Kim, H-S., Cho, K-M., Kim, W-T., "An Experimental and Computational Study of Flow Characteristics in Exhaust Manifold and CCC (Close-Coupled Catalyst)", Society of Automotive Engineers, Inc, 1998. SAE Paper No.980128.
20. Cho, Y-S., et al, "Flow Distribution in a Close-Coupled Catalytic Converter", SAE Paper No.982552
21. Wollin, J., Benjamin, S., F., "A Study of the Flow Performance of Ceramic Contoured Substrates for Automotive Exhaust Catalyst Systems" SAE Transactions, Vol. 108, Journal of Fuels and Lubricants, Section 4, pages 2014-2021, 1999
22. Shuai S-J, Wang J-X, Zhuang R-J and Chen J-R. Study on Flow Characteristics of Automotive Catalytic Converters with Various Configurations SAE paper 2000-01-0208, SP-1533 pp 41-51, 2000
23. Benjamin S. F., Roberts C. A. and Wollin J A Study of the effect of flow pulsations on the flow distribution within ceramic contoured catalyst substrates SAE 2001-01-1996, Spring F&L meeting, Orlando
24. TSI Inc. Fluid Mechanics Instrument Division, - IFA Constant Temperature Anemometer System, Instruction Manual, Part no 1990746, May 1997.
25. Mendoca J. "Close Couple Catalyst Flow Study". Final year report, Coventry University, 2000.
26. Benjamin S. F. , Haimad N, Roberts C. A. and Wollin J Modelling the flow distribution through automotive catalytic converters Proc Inst MechE, Vol 215, Part C Journal of Mechanical Sciences 2001, pp379-383.

CONTACT

Dr S. F. Benjamin
Coventry University
School of Engineering
Priory Street, Coventry
CV1 5FB, United Kingdom
email:s.benjamin@coventry.ac.uk